Mass measurements of neutron-rich gallium isotopes refine production of nuclei of the first *r*-process abundance peak in neutron-star merger calculations

M. P. Reiter,[1,2,*] S. Ayet San Andrés,[1,3,†] S. Nikas,[3,4] J. Lippuner,[5,6,7] C. Andreoiu,[8] C. Babcock,[2] B. R. Barquest,[2] J. Bollig,[2,9] T. Brunner,[2,10] T. Dickel,[1,3] J. Dilling,[2,11] I. Dillmann,[2,12] E. Dunling,[2,13] G. Gwinner,[14] L. Graham,[2] C. Hornung,[1] R. Klawitter,[2,15] B. Kootte,[2,14] A. A. Kwiatkowski,[2,12] Y. Lan,[2,11] D. Lascar,[2,16] K. G. Leach,[17] E. Leistenschneider,[2,11] G. Martínez-Pinedo,[3,4] J. E. McKay,[2,12] S. F. Paul,[2,9] W. R. Plaß,[1,3] L. Roberts,[18] H. Schatz,[7,18,19] C. Scheidenberger,[1,3] A. Sieverding,[3,4,20] R. Steinbrügge,[2,‡] R. Thompson,[21] M. E. Wieser,[21] C. Will,[1] and D. Welch[18]

[1]*II. Physikalisches Institut, Justus-Liebig-Universität, 35392 Gießen, Germany*
[2]*TRIUMF, Vancouver, British Columbia V6T 2A3, Canada*
[3]*GSI Helmholtzzentrum für Schwerionenforschung GmbH, 64291 Darmstadt, Germany*
[4]*Institut für Kernphysik (Theoriezentrum), Technische Universität Darmstadt, 64289 Darmstadt, Germany*
[5]*CCS-2, Los Alamos National Laboratory, Los Alamos, New Mexico 87545, USA*
[6]*Center for Theoretical Astrophysics, Los Alamos National Laboratory, Los Alamos, New Mexico 87545, USA*
[7]*Joint Institute for Nuclear Astrophysics, Center for the Evolution of the Elements, JINA-CEE, East Lansing, Michigan 48824, USA*
[8]*Department of Chemistry, Simon Fraser University, Burnaby, British Columbia V5A 1S6, Canada*
[9]*Ruprecht-Karls-Universität Heidelberg, D-69117 Heidelberg, Germany*
[10]*Physics Department, McGill University, H3A 2T8 Montréal, Québec, Canada*
[11]*Department of Physics and Astronomy, University of British Columbia, Vancouver, British Columbia V6T 1Z1, Canada*
[12]*Department of Physics and Astronomy, University of Victoria, Victoria, British Columbia V8P 5C2, Canada*
[13]*Department of Physics, University of York, York YO10 5DD, United Kingdom*
[14]*Department of Physics and Astronomy, University of Manitoba, Winnipeg, Manitoba R3T 2N2, Canada*
[15]*Max-Planck-Institut für Kernphysik, Heidelberg D-69117, Germany*
[16]*Center for Fundamental Physics, Northwestern University, Evanston, Illinois 60208, USA*
[17]*Department of Physics, Colorado School of Mines, Golden, Colorado 80401, USA*
[18]*National Superconducting Cyclotron Laboratory, Michigan State University, East Lansing, Michigan 48824, USA*
[19]*Department of Physics and Astronomy, Michigan State University, East Lansing, Michigan 48824, USA*
[20]*School of Physics and Astronomy, University of Minnesota, Minneapolis 55455, USA*
[21]*Department of Physics and Astronomy, University of Calgary, Calgary, Alberta T2N 1N4, Canada*

(Received 26 October 2018; revised manuscript received 25 November 2019; accepted 24 January 2020; published 10 February 2020)

We report mass measurements of neutron-rich Ga isotopes $^{80-85}$Ga with TRIUMF's Ion Trap for Atomic and Nuclear science. The measurements determine the masses of $^{80-83}$Ga in good agreement with previous measurements. The masses of ^{84}Ga and ^{85}Ga were measured for the first time. Uncertainties between 25 and 48 keV were reached. The new mass values reduce the nuclear uncertainties associated with the production of $A \approx 84$ isotopes by the *r*-process for astrophysical conditions that might be consistent with a binary neutron star (BNS) merger producing a blue kilonova. Our nucleosynthesis simulations confirm that BNS merger may contribute to the first abundance peak under moderate neutron-rich conditions with electron fractions $Y_e = 0.35$-0.38.

DOI: 10.1103/PhysRevC.101.025803

I. INTRODUCTION

Since the first discovery of a binary neutron-star (BNS) system (PSR1916 + 16) [1], the merger of two neutron stars has been considered a promising site for the production of heavy elements by the rapid neutron capture process, *r*-process [2–7]. The *r*-process in BNS mergers provides a unique electromagnetic signature known as kilonova/macronova [8–12]. Except for a few candidates, e.g., Refs. [13–17] such signatures were not clearly observed. The situation changed with the observations of the gravitational waves from the BNS merger (GW170817) [18,19] and the subsequent detection of the electromagnetic counterpart (AT2017gfo) [20]. The optical, infrared, and ultraviolet spectra and their evolution agree well with the macronova/kilonova model, constituting first direct evidence

*Present address: Institute for Particle and Nuclear Physics (IPNP), University of Edinburgh, Peter Guthrie Tait Road, EH9 3FD Edinburgh, United Kingdom; mreiter@ed.ac.uk
†Part of doctoral thesis at JLU Giessen (2018).
‡Present address: Deutsches Elektronen-Synchrotron DESY, Notkestr. 85, 22607 Hamburg, Germany.

that heavy elements, including the lanthanide region, were synthesized by the r-process [21–24]. The early blue emission [25–28], consistent with electron fractions of around $Y_e \approx 0.25$-0.4 [29–31], suggests the production of intermediate mass r-process nuclides with masses below $A < 140$. However, there has been in general no direct evidence for the production of elements of the first r-process abundance peak, except one recent study, which concludes the identification of strontium in a reanalysis of the AT2017gfo specra [32].

R-process nucleosynthesis proceeds by (n, γ) neutron captures in competition with (γ, n) photodissociation reactions and β decay. Nuclei around the closed neutron shells serve as waiting points and sensitivity studies have shown strong dependence of the final abundance pattern on nuclear masses [33–37], β-decay rates [38–40], β-delayed neutron emission [41], fission properties [42–44], (n, γ) reaction rates [40], as well as to statistical quantities like strength functions and level densities [45].

Simulations show that magnetorotational supernovae [46,47] and BNS mergers [48,49] can produce the first r-process peak under moderate entropy, entropy per nucleon $\approx 10\, k_B$/nucleon, and moderately neutron-rich conditions, electron fractions $Y_e \approx 0.35$.

To cast more light on the formation of the first r-process abundance peak and investigate whether the ejecta of a BNS merger can indeed be one of the possible sites for the formation of $A \approx 80$-84 r-process elements is of general interest. This requires BNS merger r-process simulations with accurate nuclear physics properties. The formation of the first abundance peak offers a unique opportunity for precision studies, because the r-process runs closest to stability where a majority of nuclear properties have been experimentally measured. However, to understand the synthesis of $A \approx 84$ nuclei in r-process models precise masses of neutron-rich Ga, Ni, Cu, and Zn isotopes are needed [33,34].

Here we present the first experimental results for the masses of ^{84,85}Ga. They significantly reduce the nuclear physics uncertainties for the synthesis of $A \approx 84$ nuclei in r-process models and allow a systematic investigation of the formation of the first r-process peak.

II. EXPERIMENTAL DESCRIPTION

Neutron-rich Ga isotopes were produced by a $\approx$480 MeV, 10-μA proton beam impinging on a UC_x target [50] at the ISAC facility [51]. The continuous, mass-separated beam from TRIUMF's Ion Guide Laser Ion Source (IG-LIS) [52] was accumulated and bunched in TRIUMF's Ion Trap for Atomic and Nuclear science (TITAN) Radio-Frequency-Quadrupole (RFQ) cooler-buncher [53] and ion bunches were sent to the Multiple-Reflection Time-of-Flight Mass-Spectrometer and isobar separator (MR-TOF-MS) [54–56], operated at a 20-ms cycle time. The radioactive ion beam (RIB), containing predominantly singly charged Rb, Br, and Ga, was captured in the gas-filled RFQ system of MR-TOF-MS and transported to a dedicated injection trap. Natural Rb ions from a thermal ion source were merged with the RIB via an RFQ switch yard [57] to provide independent calibration ions.

In order to reach high resolving powers the flight path is extended by storing ions for multiple reflections between two electrostatic ion mirrors [58]. The spectrometer herein is based on Refs. [59,60], using a dynamic time-focus shift [61]. The ions were kept between 330 and 372 turns in the mass analyzer resulting in flight times between 6.00 and 6.82 ms and yielding mass resolving powers of $m/\Delta m \approx 200\,000$. The number of turns was chosen such that natural Rb ions did not interfere with the RIB ions and arrive outside of the time-of-flight window of the RIB species. The ions were detected by a MultiChannelPlate (MCP) detector and the time-of-flight was recorded using a time-to-digital converter (TDC, ORTEC 9353).

III. DATA ANALYSIS

In the MR-TOF-MS, the mass of an ion is determined based on the nonrelativistic relation between the mass m, the charge q, and the time-of-flight t_{tof} needed to travel a certain flight path, resulting in $m/q = c(t_{\text{tof}} - t_0)^2$. The measured time-of-flight t_{tof} is the sum of the real time-of-flight of the ion and a constant delay t_0 caused by signal propagating times. Measuring the time-of-flight of one or more reference masses allows determination of the calibration parameters. The delay t_0 depends on the system and data acquisition and can be determined offline from an independent calibration. It was determined from $^{85}Rb^+$ and $^{87}Rb^+$ ions and amounted to $t_0 = 116(3)$ ns. For the calibration of c a dominant species from the RIB was chosen; see Table I. To account for time-of-flight drifts, resulting from temperature changes and instabilities, a time-dependent calibration was used [64].

The corresponding Ga peaks could be clearly identified by their time-of-flight and by performing a measurement with and without the resonant laser ionization step [65], shown in Fig. 1 for ^{84}Ga. To account for peak-shape-dependent effects, particular for nearby or overlapping peaks, two independent analyses were performed, using Gaussian and Lorentzian line shapes, similarly to Ref. [56]. The final error on the mass value was calculated by quadratically adding: (a) the uncertainty from the fitting algorithm, (b) the statistical uncertainty of the ion of interest, (c) the uncertainty of the calibration peak and its uncertainty reported in the AME2016 [62], and (d) a systematic uncertainty of $\delta m/m_{\text{syst}} = 3 \times 10^{-7}$ [66]. The systematic uncertainty was redetermined from accuracy measurements of $^{85}Rb^+$ and $^{87}Rb^+$. In order to eliminate possible effects from ion-ion interactions the total number of ions was kept below two detected ions per cycle.

For the ^{80,82}Ga measurements systematic effects, arising from unresolved isomeric states, had to be taken into account. An isomeric state in ^{80}Ga at 22.4 keV [67] and in the calibration species ^{82}Rb at 69 keV [68] could not be resolved. The final mass values were corrected and an additional uncertainty was added, according to the procedures in AME2016 Appendix B.1 [69].

IV. RESULTS AND DISCUSSION

The final results are summarized and compared to the values given in the AME2016 [69] in Table I. The mass

TABLE I. Mass measurements of singly charged Ga isotopes performed during this experiment using TITAN's MR-TOF-MS in comparison to the values reported in AME2016 [62]; the # indicates extrapolated values therein. In addition, the half-life taken from Ref. [63], the number of isochronus turns (IT) the Ga ions were stored in the analyzer and the respective calibration species are given.

Species	$t_{1/2}$ [63] (ms)	No. of $\mathrm{IT}_{\mathrm{Ga}}$	Calibrant	Mass $\mathrm{excess}_{\mathrm{TITAN}}$ (keV/c^2)	Mass $\mathrm{excess}_{\mathrm{AME2016}}$ (keV/c^2)	Difference (keV/c^2)
^{80}Ga[a]	1900(100)	366	^{80}Ge	−59 212(48)	−59 223.7(2.9)	−12(48)
^{81}Ga	1217(5)	373	^{81}Br	−57 616(31)	−57 628(3)	−12(31)
^{82}Ga[a]	599(2)	382	^{82}Rb[b]	−52 974(31)	−52 930.7(2.4)	43(31)
^{83}Ga	308(10)	333	^{83}Rb	−49 258(25)	−49 257.1(2.6)	1(25)
^{84}Ga	85(10)	332	^{84}Rb	−44 094(30)	−44 090(200)#	4(202)#
^{85}Ga	92(4)	360	^{85}Rb	−39 744(37)	−39 850(300)#	−106(302)#

[a]These measurements were affected by an unresolved isomeric state in either the Ga isotope of interest or the calibration species, see text for description.

[b]Assuming the measured state in ^{82}Rb is dominantly the isomer at 69 keV, as suggested by spectroscopy at ISAC Yield Station, the mass of ^{82}Ga is −52 939(23) keV/c^2.

values of ^{80,81,83}Ga agree well with the AME2016 values, which are based on measurements performed by JYFLTRAP [70]. Our result for ^{82}Ga deviates by 1.3σ from the previous measurement. Assuming the measured state in the calibration species ^{82}Rb is dominantly the isomer at an excitation energy of 69 keV, as suggested based on spectroscopy at ISAC Yield Station, the mass of ^{82}Ga results in −52 939(23) keV/c^2, which is in good agreement with the JYFLTRAP result. The masses of ^{84,85}Ga were measured for the first time and are compared to extrapolations in Table I.

Based on the mass values M, we calculate the two-neutron separation energy $S_{2\mathrm{n}}(N,Z) = M(Z,N-2)c^2 + 2M_nc^2 - M(N,Z)c^2$, with M_n the mass of the neutron, and compare it in Fig. 2 to the neighboring isotopic chains. The drop in $S_{2\mathrm{n}}$, associated with the closed neutron shell at $N = 50$, can be seen in the Ga isotopic chain [70]. The new $S_{2\mathrm{n}}$ values for ^{84,85}Ga confirm the recurrence to a smooth trend beyond the $N = 50$ shell closure and bring the Ga isotopic chain in line with the neighboring Ge and As chains.

We compare the experimental $S_{2\mathrm{n}}$ values to values based on commonly used mass models (FRDM [72], Duflo-Zucker [73], ETFSI-Q [74], and HFB-21 [75]). For the Ga isotopes in this region FRDM and HFB-21 show overall good agreement, whereas ETFSI-Q systematical predicts less binding and Duflo-Zucker overpredicts the strength of the $N = 50$ shell closure. Beyond $N = 54$, FRDM, HFB-21, and Duflo-Zucker all predict a continuation of the smooth trend.

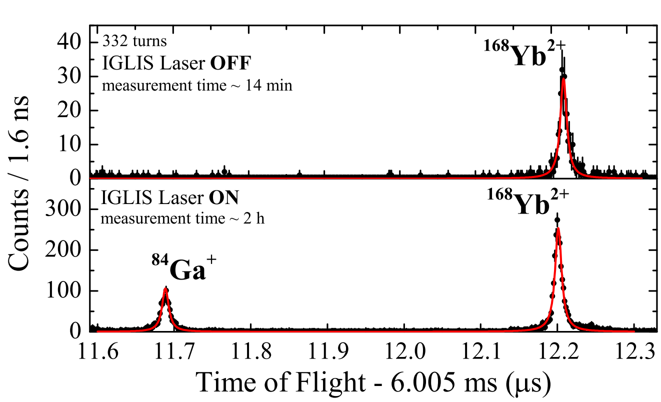

FIG. 1. Time-of-flight spectra obtained with the MR-TOF-MS around ^{84}Ga$^+$ confirming the identification of ^{84}Ga$^+$ by blocking the resonant IG-LIS laser. The lower spectra shows ≈1200 ^{84}Ga$^+$ ions from which the mass of ^{84}Ga has been determined. The red lines are fits to the data using Lorentzian peak shapes.

V. ASTROPHYSICAL IMPLICATIONS

To systematically study the formation of $A \approx 84$ nuclei, (n,γ) and (γ,n) reaction rates corresponding to the mass values of ^{84,85}Ga were calculated using the Hauser-Feshbach statistical code TALYS [76]. The resulting cross sections were initially used in two different nuclear reaction network codes, *GSINet* [35] and *SkyNet* [77], to calculate the r-process abundances. Comparing final abundances from the two network codes showed that both predict almost identical results, highlighting the robustness of the network codes themselves.

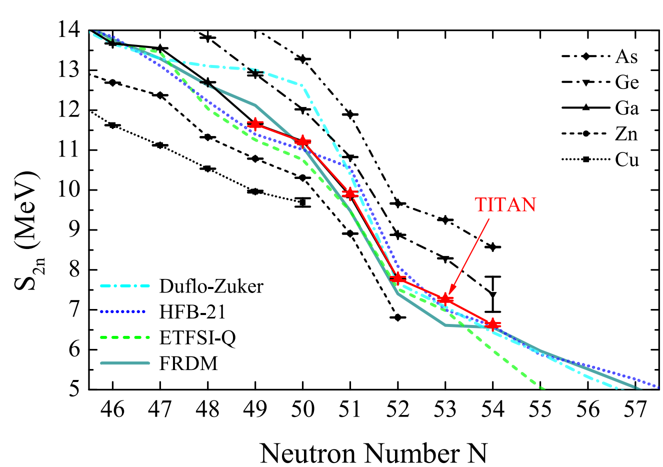

FIG. 2. Experimental two-neutron separation energies $S_{2\mathrm{n}}$ for Z = 30-33 (Zn to As) as a function of neutron number taken from AME2016 [62], including [71]. For comparison, $S_{2\mathrm{n}}$ values based on the new TITAN masses (red) and based on commonly used mass models (FRDM [72], Duflo-Zucker [73], ETFSI-Q [74], and HFB-21 [75]) are shown.

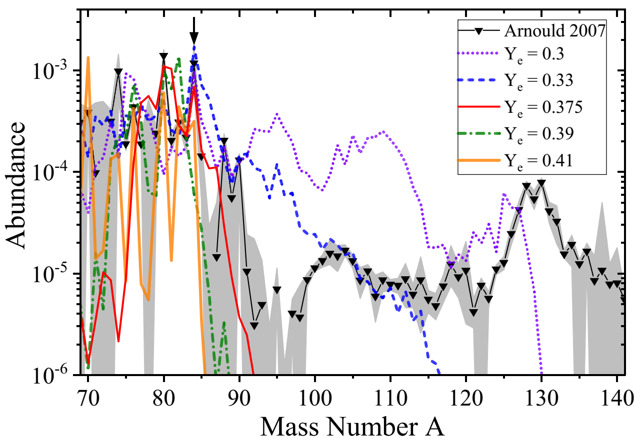

FIG. 3. Solar r-process abundance, with uncertainty shown as gray band, in comparison to the abundance resulting from neutron star merger network calculations for different Y_e using GSINet. The individual abundance curves are shown with equal weights. The r-process abundance [7] has been scaled to match the average production of ^{82}Se. The arrow indicates the $A = 84$ abundance maximum of the first r-process abundance peak.

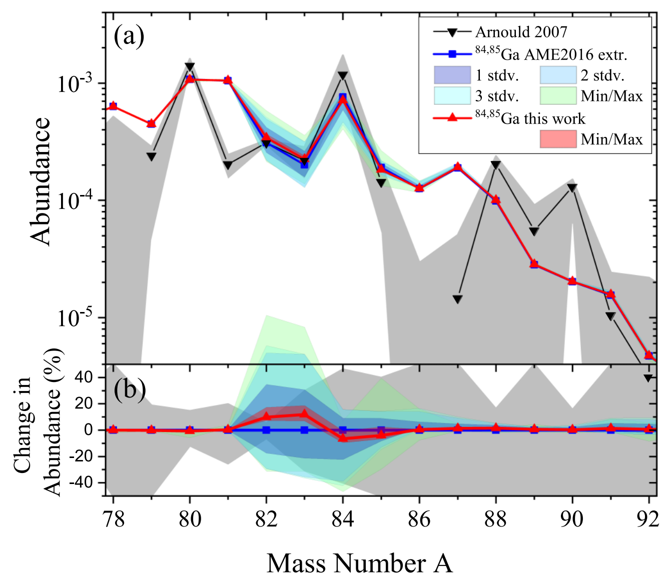

FIG. 4. (a) Final abundances averaged over calculations with $Y_e = 0.35$-0.38 compared to the solar r-process abundance [7], with uncertainty shown as gray band. The colored bands show the 1-, 2-, and 3σ change in calculated production, as well as the maximum and minimum abundance from the Monte Carlo variation of the nuclear masses of ^{84,85}Ga following a Gaussian distribution with σ of 200 and 300 keV, respectively. For the new mass values only the maximum and minimum abundance band from the variation within their uncertainty is shown. (b) Change, in percentage, of the abundance pattern as a result of using the mass values from this work compared to the extrapolations given in the AME2016.

The masses of ^{84,85}Ga modify the reaction rates around $^{83-86}$Ga; nuclei not affected were taken from JINA REACLIB [78]. Where available, experimental masses from AME2016 were used; otherwise, masses based on the FRDM mass model [72] were taken (with exception of ^{84,85}Ga). To quantify the uncertainty of the final abundance associated with the mass values of ^{84,85}Ga we use a Monte Carlo–type approach. The masses of ^{84,85}Ga were randomly varied within a normal distribution with σ according to the uncertainty of their extrapolated mass values given in the AME2016 [62]. For a set of 100 possible combinations of mass values drawn from the uncertainty distribution (n, γ) cross sections were calculated. Combinations that would result in inverted odd-even effects for the one-neutron separation energies in the Ga isotopic chain were excluded. By using each combination in a GSINet calculation an estimate for the overall uncertainty of the final abundances was obtained. The procedure was repeated using the new ^{84,85}Ga mass values and respective uncertainties.

β-decay rates and β-delayed neutron emission branches were taken from NUBASE [63], including recent measurements [71,79,80]. Otherwise, values from theoretical predictions [81] were used.

The thermodynamic evolution was parametrized assuming a free homologous expansion [48]. Starting from an initial temperature of 6 GK and entropy of 10 k_B/baryon the expansion timescale was chosen to be 7 ms. Qualitatively, our results are robust with respect to variations of the initial entropy and expansion timescale within a factor of two. We calculate the abundance after 1 Gyr for a wide range of initial Y_e between 0.28 and 0.43, consistent with the lanthanide-free ejecta of the blue kilonova.

In Fig. 3 we show a subset of these in comparison to the abundance (traditionally) assigned to the solar r-process [7], obtained by subtraction of the s-processes from the solar abundance. The abundance pattern in the region of the first r-process peak is associated with large uncertainties due to admixtures of weak- and main s-process. However, for $A = 79$ to 85 species the r-process residuals have been estimated more precisely with uncertainties of about ≈20 to 50%, see gray error band in Figs. 3 and 4. This is important for a precision study, because it allows for a fine investigation and comparison of the production with BNS merger calculations. We focus on this region, where we choose ^{82}Se as a reference isotope, because it is shielded from contributions of the s-process and requires a pure r-process source. The outstanding features in this mass region are the abundance maxima at $A = 80$ and $A = 84$.

Nucleosynthesis under neutron-rich conditions, similarly to those explored in the present work, has been studied assuming nuclear statistical equilibrium (NSE) [82]. In our full-scale network calculations we find that NSE provides a good description of the abundances for temperatures above 4.5 GK. Below this temperature the network and NSE abundance distributions result in very different peak structures. As an example, for $Y_e = 30/80 = 0.375$ NSE produces only $A = 80$ nuclei while the network produces a broader distribution of nuclei including peaks at $A = 80$, 81, and 84 (see Fig. 3). In our network calculations Y_e between 0.35 and 0.38 provide the strongest contribution to the mass region around the $A =$ 80 and $A = 84$ abundance peaks. Lower Y_e overproduce the $A = 90$-120 region by more than one order of magnitude and were therefore discarded. Y_e above 0.39 do not reach the

$A = 84$ abundance maximum, as shown in Fig. 3, or produce only reduced amounts of $A = 84$, as e.g., shown for $Y_e = 0.41$, and were not considered further.

In Fig. 4 we compare our results with the solar *r*-process abundances in the region $A \approx 80$-90. We include uncertainty bands showing the variation of the abundances arising from the error bars of the masses of ^{84,85}Ga. Calculations within $Y_e = 0.35$-0.38 were combined with equal weight.

The new ^{84,85}Ga mass values affect the abundances of elements with mass number $A = 82$-87 with the biggest impact on $A = 83$, which changes by about ≈15% despite the small change in mass value (see explanation of the formation in Sec. V A).

Furthermore, the uncertainty of the production of the *r*-process-only reference isotope ^{82}Se is significantly reduced to a level now comparable to the uncertainty of its *r*-process residual, which is crucial for drawing quantitative conclusions about the production in this region.

For combinations of mass values leading to a low neutron separation energy of ^{85}Ga, the formation of a $A = 84$ abundance peak is reduced (see lower limit error band Fig. 4). The new mass values reduce the uncertainty of the final abundance sufficiently and the formation of an abundance peak at $A = 84$ becomes plausible.

The calculations show in general a good agreement compared to the solar *r*-process abundance, particularly for the $A = 80$ and $A = 84$ abundance peaks, but a strong overproduction at $A = 81$, possibly $A = 86$ and $A = 87$, and a reduced production at $A = 90$.

A. Formation of the final abundance

The formation of the final abundance curve is illustrated by the nuclear reaction flows shown in Fig. 5 based on the calculation with $Y_e = 0.35$. They indicate the importance of β-delayed neutron emission and late time neutron captures. When taking the new mass values into account, most major nuclear physics inputs required for the formation of the $A = 84$ abundance peak in BNS mergers are now in place. This is a unique situation at the first *r*-process peak and allows for the identification of remaining key nuclei, whose masses and decay properties (half-lives and β-delayed neutron emission) are urgently needed to fully understand the possible formation of the first *r*-process peak in BNS merger calculations.

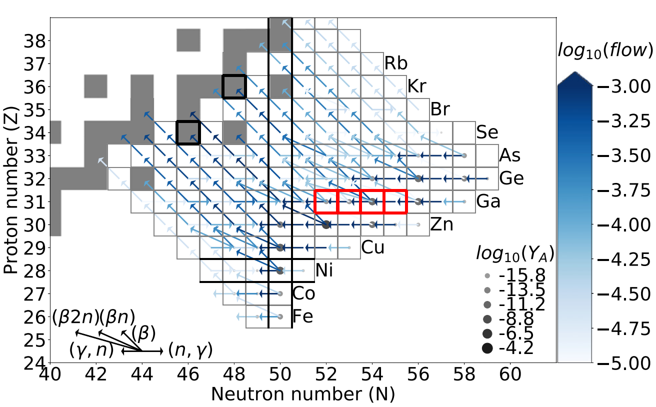

FIG. 5. Time-integrated reaction flows at $Y_e = 0.35$ from the freeze-out of the *r*-process at a neutron-to-seed ratio of unity until the final abundances are established, relevant for the nucleosynthesis in the mass regions $A = 78$-86. Most abundant nuclei at freeze-out are marked with solid circles. Gray filled squares indicate stable nuclei. Red squares indicate nuclei for which the reaction rates have been affected by the uncertainties of the mass value of ^{84}Ga and ^{85}Ga, while black ones indicate the abundance peaks at $A = 80$ and $A = 84$, corresponding to ^{80}Se and ^{84}Kr. Arrows indicate the intensity of the flow.

For the conditions considered here, the $A = 80$ (^{80}Se) peak in the solar *r*-process residuals is mainly produced at the $N = 50$ neutron magic number as ^{80}Zn in the range $Y_e \approx 0.36$–0.37. The $A = 84$ (^{84}Kr) peak is produced for the whole range of Y_e values considered with contributions from the neutron-rich Ga isotopes measured in the present work. ^{84}Ga, having an odd-neutron number and a strong β-delayed neutron emission branching of about ≈50% [79], does not contribute significantly to the final abundance of $A = 84$. The final abundance of ^{84}Kr results mostly from the decay of ^{85}Ga. ^{85}Ga is the most abundant species in the Ga isotopic chain at the freeze-out of the *r*-process as it has an even number of neutrons. Due to its high β-delayed neutron emission branching of ≈ 70% [80] it dominates the production of ^{84}Kr.

The solar *r*-process residuals for $A = 86$ (^{86}Kr) and $A = 87$ (^{87}Rb) are very uncertain, hence the differences might arise from uncertainties in the *s*-process abundance [83], which, however, can only account for some of the discrepancy. To further investigate this overproduction precise masses and β-delayed neutron emissions of ^{86,87}Ga and $^{86-88}$Ge are needed. We note that recently β-delayed neutron emissions of ^{86,87}Ga have been reported [84] but are not yet included in our calculations. Masses of more neutron-rich Ge will also confine possible production of strontium in BNS mergers [32].

The $A = 81$ (^{81}Br) abundance is produced mainly from β-delayed neutron emission of ^{82}Zn, whose half-life exhibits some inconsistencies (228(10) ms [85], 178(2.5) ms [86], 155(20) ms [87]), but, more importantly, the masses of ^{83,84}Zn, which determine the neutron capture flow beyond ^{82}Zn and therefore its freeze-out abundance, are not experimentally known and as such might alter the production of ^{81}Br.

VI. CONCLUSION

In summary, using TITAN's MR-TOF-MS we were able to measure the mass of neutron-rich Ga isotopes ^{84}Ga and ^{85}Ga for the first time with uncertainties between 25 and 48 keV. Performing *r*-process nucleosynthesis calculations for conditions possibly prevalent in the ejecta of the GW170817 BNS merger, we show how light *r*-process elements may be produced. In our BNS merger calculations electron fractions with $Y_e = 0.35$-0.38 contribute to the formation of the first *r*-process abundance peak. Under these conditions, we demonstrate that at moderate neutron-rich conditions BNS merger calculations can produce the $A = 84$ abundance feature of the solar system *r*-process residuals. Reducing nuclear physics uncertainties associated with ^{84,85}Ga isotopes is a step forward constraining nucleosynthesis of light r-process elements. In order to understand additional fine features of the abundance pattern, e.g., the production of strontium in BNS merger, additional nuclear physics uncertainties need to be addressed. In particular, nuclear masses and decay properties of more neutron-rich Ge and Zn isotopes are needed.

ACKNOWLEDGMENTS

The authors thank the TRILIS group at TRIUMF for Ga beam development and beautiful operation of the IG-LIS ion source and J. Bergmann for the Massdata-Acquisition software package used for the MR-TOF-MS, and discussions with F.-K. Thielemann are also acknowledged. This work was partially supported by Canadian agencies NSERC and CFI, U.S.A. NSF (Grants No. PHY-1419765 and No. PHY-1614130) and DOE (Grant No. DE-SC0017649), Brazil's CNPq (Grant No. 249121/2013-1), United Kingdom's STFC (Grants No. ST/L005816/1 and No. ST/L005743/1), the Canada-UK Foundation, German institutions DFG (Grants No. FR 601/3-1 and No. SFB 1245 and through PRISMA Cluster of Excellence), BMBF (Grants No. 05P15RGFN1 and No. 05P12RGFN8), the Helmholtz Association through NAVI (Grant No. VH-VI-417), HMWK through the LOEWE Center HICforFAIR, by the JLU and GSI under the JLU-GSI strategic Helmholtz partnership agreement, the ChETEC COST Action (CA16117) supported by COST (European Cooperation in Science and Technology), and the Los Alamos National Laboratory and has been assigned report number LA-UR-18-28439. Los Alamos National Laboratory is operated by Los Alamos National Security, LLC, for the National Nuclear Security Administration of US Department of Energy (Contract No. DEAC52-06NA25396). TRIUMF receives federal funding via NRC-CNRC.

[1] R. A. Hulse and J. H. Taylor, Astrophys. J. **195**, L51 (1975).
[2] J. M. Lattimer and D. N. Schramm, Astrophys. J. **192**, L145 (1974).
[3] J. M. Lattimer and D. N. Schramm, Astrophys. J. **210**, 549 (1976).
[4] D. Eichler, M. Livio, T. Piran, and D. N. Schramm, Nature **340**, 126 (1989).
[5] S. Rosswog, M. Liebendörfer, F.-K. Thielemann, M. B. Davies, W. Benz, and T. Piran, Astron. Astrophys. **341**, 499 (1999).
[6] C. Freiburghaus, S. Rosswog, and F.-K. Thielemann, Astrophys. J. Lett. **525**, L121 (1999).
[7] M. Arnould, S. Goriely, and K. Takahashi, Phys. Rep. **450**, 97 (2007).
[8] L.-X. Li and B. Paczyński, Astrophys. J. **507**, L59 (1998).
[9] B. Metzger, G. Martínez-Pinedo, S. Darbha, E. Quataert, A. Arcones, D. Kasen, R. Thomas, P. Nugent, I. Panov, and N. T. Zinner, Mon. Not. R. Astron. Soc. **406**, 2650 (2010).
[10] L. F. Roberts, D. Kasen, W. H. Lee, and E. Ramirez-Ruiz, Astrophys. J. **736**, L21 (2011).
[11] A. Bauswein, S. Goriely, and H.-T. Janka, Astrophys. J. **773**, 78 (2013).
[12] R. Fernández and B. D. Metzger, Annu. Rev. Nucl. Part. Sci. **66**, 23 (2016).
[13] D. A. Perley, B. D. Metzger, J. Granot, N. R. Butler, T. Sakamoto, E. Ramirez-Ruiz, A. J. Levan, J. S. Bloom, A. A. Miller, A. Bunker, H.-W. Chen, A. V. Filippenko, N. Gehrels, K. Glazebrook, P. B. Hall, K. C. Hurley, D. Kocevski, W. Li, S. Lopez, J. Norris, A. L. Piro, D. Poznanski, J. X. Prochaska, E. Quataert, and N. Tanvir, Astrophys. J. **696**, 1871 (2009).
[14] N. R. Tanvir, A. J. Levan, A. S. Fruchter, J. Hjorth, R. A. Hounsell, K. Wiersema, and R. L. Tunnicliffe, Nature (London) **500**, 547 (2013).
[15] E. Berger, W. Fong, and R. Chornock, Astrophys. J., Lett. **774**, L23 (2013).
[16] Z.-P. Jin, X. Li, Z. Cano, S. Covino, Y.-Z. Fan, and D.-M. Wei, Astrophys. J., Lett. **811**, L22 (2015).
[17] B. Yang, Z.-P. Jin, X. Li, S. Covino, X.-Z. Zheng, K. Hotokezaka, Y.-Z. Fan, T. Piran, and D.-M. Wei, Nat. Commun. **6**, 7323 (2015).
[18] B. P. Abbott, R. Abbott, T. Abbott, F. Acernese, K. Ackley, C. Adams, T. Adams, P. Addesso, R. Adhikari, V. Adya *et al.*, Phys. Rev. Lett. **119**, 161101 (2017).
[19] B. P. Abbott, R. Abbott, T. D. Abbott, F. Acernese, K. Ackley, C. Adams, T. Adams, P. Addesso, R. X.Adhikari *et al.*, Astrophys. J. Lett. **848**, L13 (2017).
[20] B. P. Abbott, R. Abbott, T. D. Abbott, F. Acernese, K. Ackley, C. Adams, T. Adams, P. Addesso, R. X. Adhikari, V. B. Adya *et al.*, Astrophys. J. Lett. **848**, L12 (2017).
[21] N. R. Tanvir, A. J. Levan, C. González-Fernández, O. Korobkin, I. Mandel, S. Rosswog, J. Hjorth, P. D'Avanzo, A. S. Fruchter, C. L. Fryer, T. Kangas, B. Milvang-Jensen, S. Rosetti, D. Steeghs, R. T. Wollaeger, Z. Cano, C. M. Copperwheat, S. Covino, V. D'Elia, A. de Ugarte Postigo, P. A. Evans, W. P. Even, S. Fairhurst, R. F. Jaimes, C. J. Fontes, Y. I. Fujii, J. P. U. Fynbo, B. P. Gompertz, J. Greiner, G. Hodosan, M. J. Irwin, P. Jakobsson, U. G. Jørgensen, D. A. Kann, J. D. Lyman, D. Malesani, R. G. McMahon, A. Melandri, P. T. O'Brien, J. P. Osborne, E. Palazzi, D. A. Perley, E. Pian, S. Piranomonte, M. Rabus, E. Rol, A. Rowlinson, S. Schulze, P. Sutton, C. C. Thöne, K. Ulaczyk, D. Watson, K. Wiersema, and R. A. M. J. Wijers, Astrophys. J. **848**, L27 (2017).
[22] R. Chornock, E. Berger, D. Kasen, P. S. Cowperthwaite, M. Nicholl, V. A. Villar, K. D. Alexander, P. K. Blanchard, T. Eftekhari, W. Fong, R. Margutti, P. K. G. Williams, J. Annis, D. Brout, D. A. Brown, H.-Y. Chen, M. R. Drout, B. Farr, R. J. Foley, J. A. Frieman, C. L. Fryer, K. Herner, D. E. Holz, R. Kessler, T. Matheson, B. D. Metzger, E. Quataert, A. Rest, M. Sako, D. M. Scolnic, N. Smith, and M. Soares-Santos, Astrophys. J. **848**, L19 (2017).
[23] E. Pian, P. D'Avanzo, S. Benetti, M. Branchesi, E. Brocato, S. Campana, E. Cappellaro, S. Covino, V. D'Elia, J. P. U. Fynbo, F. Getman, G. Ghirlanda, G. Ghisellini, A. Grado, G. Greco, J. Hjorth, C. Kouveliotou, A. Levan, L. Limatola, D. Malesani, P. A. Mazzali, A. Melandri, P. Møller, L. Nicastro, E. Palazzi,

S. Piranomonte, A. Rossi, O. S. Salafia, J. Selsing, G. Stratta, M. Tanaka, N. R. Tanvir, L. Tomasella, D. Watson, S. Yang, L. Amati, L. A. Antonelli, S. Ascenzi, M. G. Bernardini, M. Boër, F. Bufano, A. Bulgarelli, M. Capaccioli, P. Casella, A. J. Castro-Tirado, E. Chassande-Mottin, R. Ciolfi, C. M. Copperwheat, M. Dadina, G. De Cesare, A. Di Paola, Y. Z. Fan, B. Gendre, G. Giuffrida, A. Giunta, L. K. Hunt, G. L. Israel, Z.-P. Jin, M. M. Kasliwal, S. Klose, M. Lisi, F. Longo, E. Maiorano, M. Mapelli, N. Masetti, L. Nava, B. Patricelli, D. Perley, A. Pescalli, T. Piran, A. Possenti, L. Pulone, M. Razzano, R. Salvaterra, P. Schipani, M. Spera, A. Stamerra, L. Stella, G. Tagliaferri, V. Testa, E. Troja, M. Turatto, S. D. Vergani, and D. Vergani, Nature **551**, 67 (2017).

[24] D. Kasen, B. Metzger, J. Barnes, E. Quataert, and E. Ramirez-Ruiz, Nature **551**, 80 (2017).

[25] P. Evans, S. Cenko, J. Kennea, S. Emery, N. Kuin, O. Korobkin, R. Wollaeger, C. Fryer, K. Madsen, F. Harrison *et al.*, Science **358**, 1565 (2017).

[26] S. J. Smartt, T.-W. Chen, A. Jerkstrand, M. Coughlin, E. Kankare, S. A. Sim, M. Fraser, C. Inserra, K. Maguire, K. C. Chambers *et al.*, Nature **551**, 75 (2017).

[27] E. Troja, G. Ryan, L. Piro, H. van Eerten, S. B. Cenko, Y. Yoon, S.-K. Lee, M. Im, T. Sakamoto, P. Gatkine, A. Kutyrev, and S. Veilleux, Nat. Commun. **9**, 4089 (2018).

[28] M. Nicholl, E. Berger, D. Kasen, B. D. Metzger, J. Elias, C. Briceño, K. D. Alexander, P. K. Blanchard, R. Chornock, P. S. Cowperthwaite, T. Eftekhari, W. Fong, R. Margutti, V. A. Villar, P. K. G. Williams, W. Brown, J. Annis, A. Bahramian, D. Brout, D. A. Brown, H.-Y. Chen, J. C. Clemens, E. Dennihy, B. Dunlap, D. E. Holz, E. Marchesini, F. Massaro, N. Moskowitz, I. Pelisoli, A. Rest, F. Ricci, M. Sako, M. Soares-Santos, and J. Strader, Astrophys. J. **848**, L18 (2017).

[29] S. Rosswog, J. Sollerman, U. Feindt, A. Goobar, O. Korobkin, R. Wollaeger, C. Fremling, and M. M. Kasliwal, Astron. Astrophys. **615**, A132 (2018).

[30] S. Wanajo, Astrophys. J. **868**, 65 (2018).

[31] M.-R. Wu, J. Barnes, G. Martinez-Pinedo, and B. D. Metzger, Phys. Rev. Lett. **122**, 062701 (2019).

[32] D. Watson, C. J. Hansen, J. Selsing, A. Koch, D. B. Malesani, A. C. Andersen, J. P. Fynbo, A. Arcones, A. Bauswein, S. Covino *et al.*, Nature **574**, 497 (2019).

[33] S. Brett, I. Bentley, N. Paul, R. Surman, and A. Aprahamian, Eur. Phys. J. A **48**, 184 (2012).

[34] A. Aprahamian, I. Bentley, M. Mumpower, and R. Surman, AIP Adv. **4**, 041101 (2014).

[35] J. J. Mendoza-Temis, M.-R. Wu, K. Langanke, G. Martínez-Pinedo, A. Bauswein, and H.-T. Janka, Phys. Rev. C **92**, 055805 (2015).

[36] M. R. Mumpower, R. Surman, D. Fang, M. Beard, and A. Aprahamian, J. Phys. G: Nucl. Part. Phys. **42**, 034027 (2015).

[37] M. R. Mumpower, R. Surman, D.-L. Fang, M. Beard, P. Möller, T. Kawano, and A. Aprahamian, Phys. Rev. C **92**, 035807 (2015).

[38] M. Mumpower, J. Cass, G. Passucci, R. Surman, and A. Aprahamian, AIP Adv. **4**, 041009 (2014).

[39] T. Marketin, L. Huther, and G. Martínez-Pinedo, Phys. Rev. C **93**, 025805 (2016).

[40] M. Mumpower, R. Surman, G. McLaughlin, and A. Aprahamian, Prog. Part. Nucl. Phys. **86**, 86 (2016).

[41] K.-L. Kratz, J.-P. Bitouzet, F.-K. Thielemann, P. Moeller, and B. Pfeiffer, Astrophys. J. **403**, 216 (1993).

[42] M. Eichler, A. Arcones, A. Kelic, O. Korobkin, K. Langanke, T. Marketin, G. Martinez-Pinedo, I. Panov, T. Rauscher, S. Rosswog, C. Winteler, N. T. Zinner, and F.-K. Thielemann, Astrophys. J. **808**, 30 (2015).

[43] S. Goriely, Eur. Phys. J. A **51**, 22 (2015).

[44] S. A. Giuliani, G. Martínez-Pinedo, and L. M. Robledo, Phys. Rev. C **97**, 034323 (2018).

[45] S. Nikas, M. Beard, G. Perdikakis, R. Surman, M. Mumpower, and P. Tsintari (unpublished).

[46] C. Winteler, R. Käppeli, A. Perego, A. Arcones, N. Vasset, N. Nishimura, M. Liebendörfer, and F.-K. Thielemann, Astrophys. J. **750**, L22 (2012).

[47] N. Nishimura, T. Takiwaki, and F.-K. Thielemann, Astrophys. J. **810**, 109 (2015).

[48] J. Lippuner and L. F. Roberts, Astrophys. J. **815**, 82 (2015).

[49] D. Martin, A. Perego, A. Arcones, F.-K. Thielemann, O. Korobkin, and S. Rosswog, Astrophys. J. **813**, 2 (2015).

[50] P. Kunz, P. Bricault, M. Dombsky, N. Erdmann, V. Hanemaayer, J. Wong, and K. Lützenkirchen, J. Nucl. Mater. **440**, 110 (2013).

[51] M. Dombsky, D. Bishop, P. Bricault, D. Dale, A. Hurst, K. Jayamanna, R. Keitel, M. Olivo, P. Schmor, and G. Stanford, Rev. Sci. Instrum. **71**, 978 (2000).

[52] S. Raeder, H. Heggen, J. Lassen, F. Ames, D. Bishop, P. Bricault, P. Kunz, A. Mojs, and A. Teigelhoefer, Rev. Sci. Instrum. **85**, 33309 (2014).

[53] T. Brunner, M. J. Smith, M. Brodeur, S. Ettenauer, R. Gallino, V. V. Simon, A. Chaudhuri, A. Lapierre, E. Mané, R. Ringle, M. C. Simon, J. A. Vaz, P. Delheij, M. Good, M. R. Pearson, and J. Dilling, Nucl. Instrum. Methods A **676**, 32 (2012).

[54] C. Jesch, T. Dickel, W. R. Plass, D. Short, S. Ayet San Andres, J. Dilling, H. Geissel, F. Greiner, J. Lang, K. G. Leach, W. Lippert, C. Scheidenberger, and M. I. Yavor, Hyperfine Interact. **235**, 97 (2015).

[55] E. Leistenschneider, M. P. Reiter, S. Ayet San Andrés, B. Kootte, J. D. Holt, P. Navrátil, C. Babcock, C. Barbieri, B. R. Barquest, J. Bergmann, J. Bollig, T. Brunner, E. Dunling, A. Finlay, H. Geissel, L. Graham, F. Greiner, H. Hergert, C. Hornung, C. Jesch, R. Klawitter, Y. Lan, D. Lascar, K. G. Leach, W. Lippert, J. E. McKay, S. F. Paul, A. Schwenk, D. Short, J. Simonis, V. Somà, R. Steinbrügge, S. R. Stroberg, R. Thompson, M. E. Wieser, C. Will, M. Yavor, C. Andreoiu, T. Dickel, I. Dillmann, G. Gwinner, W. R. Plaß, C. Scheidenberger, A. A. Kwiatkowski, and J. Dilling, Phys. Rev. Lett. **120**, 062503 (2018).

[56] M. P. Reiter, S. Ayet San Andrés, E. Dunling, B. Kootte, E. Leistenschneider, C. Andreoiu, C. Babcock, B. R. Barquest, J. Bollig, T. Brunner, I. Dillmann, A. Finlay, G. Gwinner, L. Graham, J. D. Holt, C. Hornung, C. Jesch, R. Klawitter, Y. Lan, D. Lascar, J. E. McKay, S. F. Paul, R. Steinbrügge, R. Thompson, J. L. Tracy, M. E. Wieser, C. Will, T. Dickel, W. R. Plaß, C. Scheidenberger, A. A. Kwiatkowski, and J. Dilling, Phys. Rev. C **98**, 024310 (2018).

[57] W. R. Plass, T. Dickel, S. S. A. S. Andres, J. Ebert, F. Greiner, C. Hornung, C. Jesch, J. Lang, W. Lippert, T. Majoros, D. Short, H. Geissel, E. Haettner, M. P. Reiter, A.-K. A.-K. A.-K. Rink, C. Scheidenberger, and M. I. M. M. I. Yavor, Phys. Scr. **T166**, 014069 (2015).

[58] H. Wollnik and M. Przewloka, Int. J. Mass Spectrom. Ion Process. **96**, 267 (1990).

[59] M. I. Yavor, W. R. Plass, T. Dickel, H. Geissel, and C. Scheidenberger, Int. J. Mass Spectrom. **381-382**, 1 (2015).

[60] T. Dickel, W. R. Plass, A. Becker, U. Czok, H. Geissel, E. Haettner, C. Jesch, W. Kinsel, M. Petrick, C. Scheidenberger, A. Simon, and M. I. Yavor, Nucl. Instrum. Methods A **777**, 172 (2015).
[61] T. Dickel, M. I. Yavor, J. Lang, W. R. Plass, W. Lippert, H. Geissel, and C. Scheidenberger, Int. J. Mass Spectrom. **412**, 1 (2017).
[62] M. Wang, G. Audi, F. Kondev, W. Huang, S. Naimi, and X. Xu, Chin. Phys. C **41**, 030003 (2017).
[63] G. Audi, F. Kondev, M. Wang, W. Huang, and S. Naimi, Chin. Phys. C **41**, 030001 (2017).
[64] S. Ayet San Andres, C. Hornung, J. Ebert, W. R. Plass, T. Dickel, H. Geissel, C. Scheidenberger, J. Bergmann, F. Greiner, E. Haettner, C. Jesch, W. Lippert, I. Mardor, I. Miskun, Z. Patyk, S. Pietri, A. Pihktelev, S. Purushothaman, M. P. Reiter, A.-K. Rink, H. Weick, M. I. Yavor, S. Bagchi, V. Charviakova, P. Constantin, M. Diwisch, A. Finlay, S. Kaur, R. Knöbel, J. Lang, B. Mei, I. D. Moore, J.-H. Otto, I. Pohjalainen, A. Prochazka, C. Rappold, M. Takechi, Y. K. Tanaka, J. S. Winfield, and X. Xu, Phys. Rev. C **99**, 064313 (2019).
[65] R. Li, J. Lassen, A. Teigelhöfer, J. Lavoie, P. Bricault, O. Chackakova, J. Meissner, and Y. Zlateva, Nucl. Instrum. Methods B **308**, 74 (2013).
[66] C. Will, TITANs multiple-reflection time-of-flight mass spectrometer and isobar separator—Characterization and first experiments, B.Sc. thesis, University of Giessen, 2017.
[67] D. Verney, B. Tastet, K. Kolos, F. Le Blanc, F. Ibrahim, M. Cheikh Mhamed, E. Cottereau, P. V. Cuong, F. Didierjean, G. Duchêne, S. Essabaa, M. Ferraton, S. Franchoo, L. H. Khiem, C. Lau, J.-F. Le Du, I. Matea, B. Mouginot, M. Niikura, B. Roussière, I. Stefan, D. Testov, and J.-C. Thomas, Phys. Rev. C **87**, 054307 (2013).
[68] Ya. Vrzal, B. S. Czhelepov, A. G. Dmitriev, N. N. Zhukovskii, Ya. Liptak, L. N. Moskvin, Ya. Urbanets, and L. G. Tsaritsyna, Izv. Akad. Nauk SSSR, Ser. Fiz. **31**, 1661 (1967).
[69] W. J. Huang, G. Audi, M. Wang, F. G. Kondev, S. Naimi, and X. Xu, Chinese Phys. C **41**, 030002 (2017).
[70] J. Hakala, S. Rahaman, V.-V. Elomaa, T. Eronen, U. Hager, A. Jokinen, A. Kankainen, I. D. Moore, H. Penttilä, S. Rinta-Antila, J. Rissanen, A. Saastamoinen, T. Sonoda, C. Weber, and J. Äystö, Phys. Rev. Lett. **101**, 052502 (2008).
[71] A. Welker, N. A. S. Althubiti, D. Atanasov, K. Blaum, T. E. Cocolios, F. Herfurth, S. Kreim, D. Lunney, V. Manea, M. Mougeot, D. Neidherr, F. Nowacki, A. Poves, M. Rosenbusch, L. Schweikhard, F. Wienholtz, R. N. Wolf, and K. Zuber, Phys. Rev. Lett. **119**, 192502 (2017).
[72] P. Moeller, A. Sierk, T. Ichikawa, and H. Sagawa, At. Data Nucl. Data Tables **109-110**, 1 (2016).
[73] J. Duflo and A. P. Zuker, Phys. Rev. C **52**, R23(R) (1995).
[74] J. Pearson, R. Nayak, and S. Goriely, Phys. Lett. B **387**, 455 (1996).
[75] S. Goriely, N. Chamel, and J. M. Pearson, Phys. Rev. C **88**, 024308 (2013).
[76] A. J. Koning, S. Hilaire, and M. C. Duijvestijn, in *Proceedings of the International Conference on Nuclear Data for Science and Technology* (EDP Sciences, Paris, France, 2007), pp. 211–214.
[77] J. Lippuner and L. F. Roberts, Astrophys. J. Suppl. **233**, 18 (2017).
[78] R. H. Cyburt, A. M. Amthor, R. Ferguson, Z. Meisel, K. Smith, S. Warren, A. Heger, R. Hoffman, T. Rauscher, A. Sakharuk *et al.*, Astrophys. J., Suppl. Ser. **189**, 240 (2010).
[79] D. Verney, D. Testov, F. Ibrahim, Y. Penionzhkevich, B. Roussière, V. Smirnov, F. Didierjean, K. Flanagan, S. Franchoo, E. Kuznetsova, R. Li, B. Marsh, I. Matea, H. Pai, E. Sokol, I. Stefan, and D. Suzuki, Phys. Rev. C **95**, 054320 (2017).
[80] K. Miernik, K. P. Rykaczewski, R. Grzywacz, C. J. Gross, M. Madurga, D. Miller, D. W. Stracener, J. C. Batchelder, N. T. Brewer, A. Korgul, C. Mazzocchi, A. J. Mendez, Y. Liu, S. V. Paulauskas, J. A. Winger, M. Wolinska-Cichocka, and E. F. Zganjar, Phys. Rev. C **97**, 054317 (2018).
[81] P. Möller, B. Pfeiffer, and K.-L. Kratz, Phys. Rev. C **67**, 055802 (2003).
[82] D. Hartmann, S. E. Woosley, and M. F. El Eid, Astrophys. J. **297**, 837 (1985).
[83] G. Cescutti, R. Hirschi, N. Nishimura, J. W. d. Hartogh, T. Rauscher, A. S. J. Murphy, and S. Cristallo, Mon. Not. R. Astron. Soc. **478**, 4101 (2018).
[84] R. Yokoyama, R. Grzywacz, B. C. Rasco, N. Brewer, K. P. Rykaczewski, I. Dillmann, J. L. Tain, S. Nishimura, D. S. Ahn, A. Algora, J. M. Allmond, J. Agramunt, H. Baba, S. Bae, C. G. Bruno, R. Caballero-Folch, F. Calvino, P. J. Coleman-Smith, G. Cortes, T. Davinson, C. Domingo-Pardo, A. Estrade, N. Fukuda, S. Go, C. J. Griffin, J. Ha, O. Hall, L. J. Harkness-Brennan, J. Heideman, T. Isobe, D. Kahl, M. Karny, T. Kawano, L. H. Khiem, T. T. King, G. G. Kiss, A. Korgul, S. Kubono, M. Labiche, I. Lazarus, J. Liang, J. Liu, G. Lorusso, M. Madurga, K. Matsui, K. Miernik, F. Montes, A. I. Morales, P. Morrall, N. Nepal, R. D. Page, V. H. Phong, M. Piersa, M. Prydderch, V. F. E. Pucknell, M. M. Rajabali, B. Rubio, Y. Saito, H. Sakurai, Y. Shimizu, J. Simpson, M. Singh, D. W. Stracener, T. Sumikama, R. Surman, H. Suzuki, H. Takeda, A. Tarifeño Saldivia, S. L. Thomas, A. Tolosa-Delgado, M. Wolinska-Cichocka, P. J. Woods, and X. X. Xu, Phys. Rev. C **100**, 031302 (2019).
[85] M. Madurga, R. Surman, I. N. Borzov, R. Grzywacz, K. P. Rykaczewski, C. J. Gross, D. Miller, D. W. Stracener, J. C. Batchelder, N. T. Brewer, L. Cartegni, J. H. Hamilton, J. K. Hwang, S. H. Liu, S. V. Ilyushkin, C. Jost, M. Karny, A. Korgul, W. Królas, A. Kuźniak, C. Mazzocchi, A. J. Mendez, K. Miernik, S. W. Padgett, S. V. Paulauskas, A. V. Ramayya, J. A. Winger, M. Wolińska-Cichocka, and E. F. Zganjar, Phys. Rev. Lett. **109**, 112501 (2012).
[86] Z. Y. Xu, S. Nishimura, G. Lorusso, F. Browne, P. Doornenbal, G. Gey, H.-S. Jung, Z. Li, M. Niikura, P.-A. Söderström, T. Sumikama, J. Taprogge, Z. Vajta, H. Watanabe, J. Wu, A. Yagi, K. Yoshinaga, H. Baba, S. Franchoo, T. Isobe, P. R. John, I. Kojouharov, S. Kubono, N. Kurz, I. Matea, K. Matsui, D. Mengoni, P. Morfouace, D. R. Napoli, F. Naqvi, H. Nishibata, A. Odahara, E. Şahin, H. Sakurai, H. Schaffner, I. G. Stefan, D. Suzuki, R. Taniuchi, and V. Werner, Phys. Rev. Lett. **113**, 032505 (2014).
[87] M. F. Alshudifat, R. Grzywacz, M. Madurga, C. J. Gross, K. P. Rykaczewski, J. C. Batchelder, C. Bingham, I. N. Borzov, N. T. Brewer, L. Cartegni, A. Fijałkowska, J. H. Hamilton, J. K. Hwang, S. V. Ilyushkin, C. Jost, M. Karny, A. Korgul, W. Królas, S. H. Liu, C. Mazzocchi, A. J. Mendez, K. Miernik, D. Miller, S. W. Padgett, S. V. Paulauskas, A. V. Ramayya, D. W. Stracener, R. Surman, J. A. Winger, M. Wolińska-Cichocka, and E. F. Zganjar, Phys. Rev. C **93**, 044325 (2016).